Analysis of Reset Discharge Characteristics in AC-Plasma Display Panel With Various Sustain Gaps Using V_t Close-Curve

Ki-Hyung Park, Heung-Sik Tae, *Senior Member, IEEE*, and Jeong Hyun Seo

***Abstract*—The effects of various sustain gaps on the reset discharge characteristics, particularly the discharge stability, are examined based on a V_t close-curve analysis. The V_t close-curve analysis shows that the reset discharge region producing a stable discharge under an MgO cathode condition is reduced in proportion to the increase in the sustain gap, resulting in discharge instability when a conventional reset waveform is applied with a wide-sustain-gap (over 200 μm) structure. Based on the V_t close-curve analysis, a modified reset waveform suitable for a wide-sustain-gap ($= 200$ μm) structure is proposed to prevent an unstable discharge. The effects of two parameters $V_{\text{add-bias}}$ and $V_{\text{com-bias}}$ in the modified reset waveform on the reset discharge as well as the address and first sustain discharges, are examined in detail.**

***Index Terms*—Discharge stability, modified reset waveform, various sustain gaps, V_t close-curve analysis, wide-sustain-gap of 200 μm.**

I. Introduction

MANY RECENT research has focused on wide-sustain-gap (> 150 μm) structures in an effort to improve the luminance efficacy of ac-plasma display panels (PDPs). Since luminance efficacy is mainly related to the sustain discharge, most of such research has concentrated on improving the sustain discharge characteristics [1]–[8]. In ac-PDPs with a wide-sustain-gap, the characteristics of the reset discharge generated by a ramp pulse are often neglected, although the stable initialization of the millions of microdischarge cells under a low background luminance is a very important factor for displaying high quality images on a PDP. In the conventional short sustain gap structure whose sustain gap is smaller than the barrier rib height, the reset discharge is stably produced as follows: During the ramp-up period, the surface discharge is dominantly produced under an MgO cathode condition, and the ensuing plate-gap discharge is weakly produced under a phosphor cathode condition. However, in the wide-sustain-gap structure whose sustain gap is larger than the barrier rib height, the reset discharge tends to be produced unstably because the plate-gap discharge is easily produced instead of the surface discharge. Here, an MgO cathode condition means the electrodes covered with the MgO layer work as a cathode electrode during the discharge, whereas a phosphor cathode condition means the electrode covered with the phosphor layer works as a cathode electrode during the discharge. The stability of the discharge, particularly stability of the weak discharge such as a reset discharge, strongly depends on the secondary electron emission capability of the cathode electrode. Such an unstable reset discharge then causes undesirable discharge problems, such as an unstable background luminance and misfiring problems in address or sustain periods, which eventually deteriorate the image quality on an ac-PDP. Furthermore, for the on-cells, the address discharge characteristics strongly depend on the reset discharge [9]–[18]. Our previous result has already shown the effects of various sustain gaps on the reset discharge characteristics of ac-PDPs [19]. In addition to previous result, this paper has more focused on the weak reset discharge stability in a sustain gap of 200 μm. In particular, the effects of the reset discharge stability on the subsequent address discharge, including the first and second sustain discharges, are investigated in detail when applying the modified reset waveform.

This paper uses a V_t close-curve analysis first to verify the cathode condition change in the cells with various sustain gaps, such as 50, 100, 200, and 400 μm, and then to design a modified reset waveform to compensate for the weakness of surface discharge with a 200 μm wide-sustain-gap [20]–[24]. Based on a V_t close-curve analysis, various reset waveforms that can prevent an unstable reset discharge are examined with a 200 μm wide-sustain-gap, along with the detailed effects of two parameters $V_{\text{add-bias}}$ and $V_{\text{com-bias}}$ on the reset discharge characteristics with such a wide gap ($= 200$ μm). Finally, the effects of the same two parameters $V_{\text{add-bias}}$ and $V_{\text{com-bias}}$ on the address discharge and the first and second sustain discharge characteristics are also examined. Here, $V_{\text{add-bias}}$ is the voltage applied to the address (A) electrode during the ramp set-up period, while $V_{\text{com-bias}}$ is the voltage applied to the common (X) electrode during the ramp set-down period.

Manuscript received April 2, 2008. This work was supported in part by the New Growth Engine project of the Ministry of Commerce, Industry and Energy of Korea and in part by the Brain Korea 21 (BK21). The review of this paper was arranged by Editor D. Verret.

K.-H. Park and H.-S. Tae are with the School of Electrical Engineering and Computer Science, Kyungpook National University, Daegu 702-701, Korea (e-mail: hstae@ee.knu.ac.kr).

J. H. Seo is with the Department of Electronics Engineering, Incheon University, Incheon 402-751, Korea.

Color versions of one or more of the figures in this paper are available online at http://ieeexplore.ieee.org.

Digital Object Identifier 10.1109/TED.2008.927947

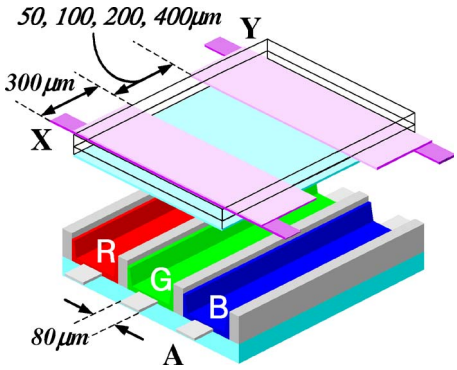

Fig. 1. PDP pixel structure with various gaps between X and Y electrodes employed in this paper.

TABLE I
SPECIFICATIONS OF 7-in TEST PANEL EMPLOYED IN THIS PAPER

Front Panel		Rear Panel	
ITO width	300 μm	Barrier rib width	55 μm
Sustain gaps	50, 100, 200, 400 μm	Barrier rib height	125 μm
		Address width	80 μm
Bus width	50 μm	Red phosphor	$(Y,Gd)BO_3$:Eu
Dielectric	30 μm	Green phosphor	$(Zn,Mn)_2SIO_4$
MgO	5000 Å	Blue phosphor	$(Ba,Eu)MgAl_{10}O_{17}$
Cell pitch	1080 μm × 360 μm		
Barrier rib	Stripe rib		
Gas chemistry	Ne-Xe (5 %)		
Gas pressure	500 Torr		

II. V_t Close Curves Measured With Various Sustain Gap Structures and Related Unstable Weak Discharge Region

Fig. 1 shows a schematic configuration of a single pixel in a 7-in test panel and the three related electrodes, X, Y, and A, where X and Y are the common (or sustain) and scan electrodes, respectively, and A is the address electrode. The plate-gap between the X (or Y) and A electrodes, i.e., the barrier rib height, was fixed at 125 μm, while the sustain gaps between the X–Y electrodes were 50, 100, 200, and 400 μm, respectively. An MgO layer with a higher secondary electron emission coefficient was deposited on the X and Y electrodes, while a phosphor layer with a lower secondary electron emission coefficient was deposited on the A electrode. The detailed specifications for the 7-in test panel are given in Table I.

Fig. 2 shows the V_t close-curves measured from the 7-in test panel used in this paper on the cell voltage plane. In Fig. 2(a), the V_t close-curve with six sides shows the breakdown threshold voltage for producing a weak discharge among the three electrodes, X, Y, and A. Each side in the V_t close-curve represents the firing threshold voltage between two electrodes. As shown in Fig. 2, as the sustain gap between the X–Y electrodes became wider, sides with V_{tXY} and V_{tYX} became narrower, and the associated firing voltages V_{tXY} and V_{tYX} increased [25]. In particular, as shown in Fig. 2(d), sides with V_{tXY} and V_{tYX} disappeared when the sustain gap between the X–Y electrodes was 400 μm, meaning that no surface discharge could directly be generated between the X–Y electrodes with a sustain gap over 400 μm. As such, a strong sustain discharge

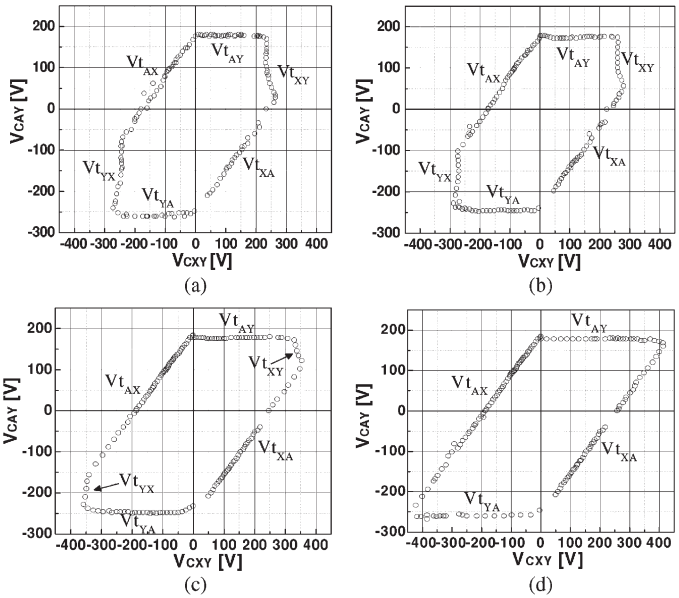

Fig. 2. V_t close-curves measured from 7-in test panel with various sustain gaps of (a) 50, (b) 100, (c) 200, and (d) 400 μm where V_{tXY} is threshold firing voltage between X–Y electrodes, V_{tAY} is threshold firing voltage between A–Y electrodes, V_{tAX} is threshold firing voltage between A–X electrodes, V_{tYX} is threshold firing voltage between Y–X electrodes, V_{tYA} is threshold firing voltage between Y–A electrodes, and V_{tXA} is threshold firing voltage between X–A electrodes.

between the X–Y electrodes could only be produced with the help of a plate-gap trigger discharge between the X (or Y)–A electrodes [4], [7]. Meanwhile, sides with V_{tAY}, V_{tAX}, V_{tYA}, and V_{tXA} became wider in proportion to an increase in the sustain gap, however, the breakdown voltages V_{tAY} (about 180 V), V_{tAX} (about 180 V), V_{tYA} (about 250 V), and V_{tXA} (about 250 V) changed little, as the gaps between the X (or Y)–A electrodes were fixed at 125 μm. In sides with V_{tAY} and V_{tAX}, the X and Y electrodes covered with the MgO layer with a higher secondary electron emission coefficient acted as the cathode, whereas in sides with V_{tYA} and V_{tXA}, the A electrode covered with the phosphor layer acted as a cathode. As a result, the breakdown voltages V_{tAY} and V_{tAX} were smaller than those V_{tYA} and V_{tXA}.

Fig. 3(a) shows the test waveforms with ramp pulses applied to the three electrodes for producing the XY, AY, YX, and YA discharges, respectively, in a wide-sustain-gap of 200 μm. When the test waveforms in Fig. 3(a) were applied, Fig. 3(b) shows the corresponding voltage vectors exceeded the threshold voltage contours of the V_t close-curves (i.e., (b)-(i) V_{tXY}, (b)-(ii) V_{tAY}, (b)-(iii) V_{tYX}, and (b)-(iv) V_{tYA}). Fig. 3(c) shows the changes in the infrared (IR) emission intensities when the ramp pulses were applied and corresponding cell voltage vectors exceeded each side. In sides with V_{tXY}, V_{tAY}, and V_{tYX}, under the MgO cathode condition, stable IR waveforms were observed, as shown in Fig. 3(c)-(i), -(ii), and -(iii). However, in side with V_{tYA}, an unstable IR emission waveform emitted from an unstable weak discharge was observed, as shown in Fig. 3(c)-(iv), as the address electrode covered by the phosphor layer acted as the cathode electrode. Since a secondary electron emission was facilitated under the MgO cathode condition, this produced a stable reset weak discharge, as shown in

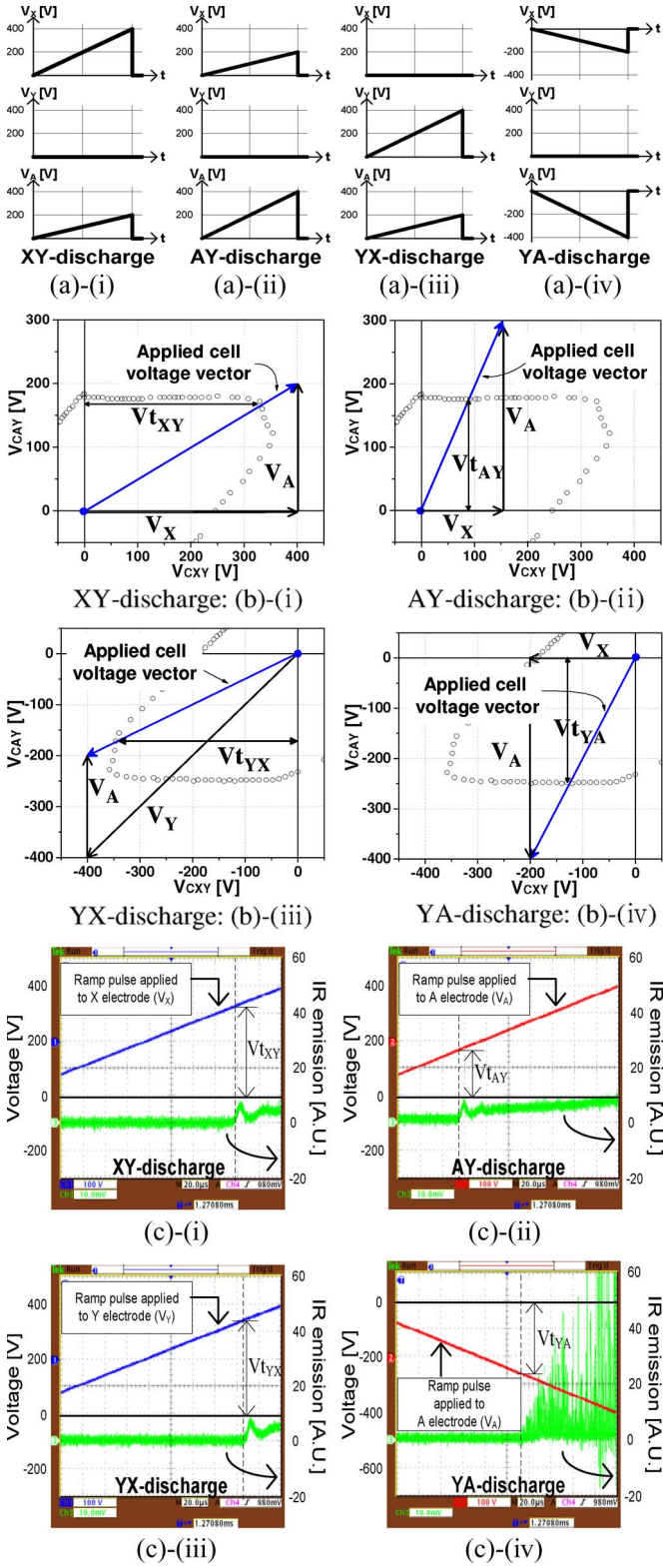

Fig. 3. (a) Test voltage waveforms for producing (a)-(i) XY-discharge, (a)-(ii) AY-discharge, (a)-(iii) YX-discharge, and (a)-(iv) YA-discharge, applied to each electrode and (b) V_t close-curves with corresponding cell voltage vectors, and (c) changes in IR emission intensities when cell voltage vector exceeded (c)-(i) V_{tXY}, (c)-(ii) V_{tAY}, (c)-(iii) V_{tYX}, and (c)-(iv) V_{tYA} with 200 μm sustain gap.

Fig. 3(a)–(c) [26]. In contrast, since the secondary-electron-emission characteristic of the phosphor layer was very poor, the weak reset discharge generated under the phosphor cathode

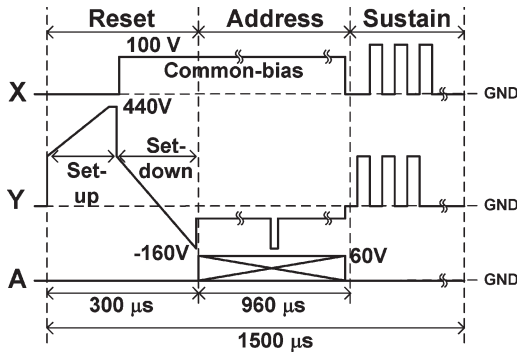

Fig. 4. Subfield driving waveform used in this paper to test reset discharge characteristics under various sustain gap conditions.

condition became unstable, along with a higher breakdown voltage, as shown in Fig. 3(b)-(iv) and (c)-(iv).

III. Modified Reset Waveform for Stable Reset Discharge With Wide-Sustain-Gap

A. Two Parameters in Modified Reset Waveform: $V_{\mathrm{add\text{-}bias}}$ and $V_{\mathrm{com\text{-}bias}}$

Fig. 4 shows the conventional driving waveform employed to examine the instability of the reset discharge relative to various sustain gaps of 50, 100, 200, and 400 μm. To remove the effect of the amplitude of the reset waveform, a sufficient voltage level was applied to the Y electrode, based on a set-up voltage of 440 V and set-down voltage of -160 V. The amplitude of the address pulse was 60 V, while the reset and address periods were 300 and 960 μs, respectively. The amplitudes of the sustain waveforms differed due to the different firing voltage conditions between the two sustain electrodes. The driving waveform in Fig. 4 was applied to the test panel with various sustain gaps of 50, 100, 200, and 400 μm under the off-cell condition.

Fig. 5(a)-(i), (b)-(i), (c)-(i), and (d)-(i) shows the trajectories of the cell voltage vectors generated by the set-up ramp pulse of 440 V displayed on the V_t close-curves in the cell voltage plane when no sustain discharge was produced in the previous state. The initial point of the cell voltage vector during a reset period is set by the previous wall voltage among the three electrodes. Thus, under a no address condition, the previous wall voltage condition was determined by the XY–AY simultaneous discharge point and applied voltages of the preceding reset discharge, i.e., the set-down (Y electrode) and common bias (X electrode) voltages [20], [21]. Therefore, when the same reset driving waveforms with a set-down of -160 V and common bias of 100 V were applied to the cells with 50, 100, 200, and 400 μm sustain gaps, the initial points shifted to the right, due to the shift of the XY–AY simultaneous discharge point to the right in proportion to the wide sustain gap, plus V_{tXY} also increased. By applying a sufficient set-up voltage to the Y electrode, the cell voltage vector exceeded the threshold voltage contours of the V_t close-curves, as shown in Fig. 5(a)-(i), (b)-(i), (c)-(i), and (d)-(i). For the 50 and 100 μm sustain gaps, the voltage vector exceeded V_{tYX} in the V_t close-curve, as shown in Fig. 5(a)-(i) and (b)-(i), meaning that the X electrode protected by the MgO layer acted as the cathode, and a stable

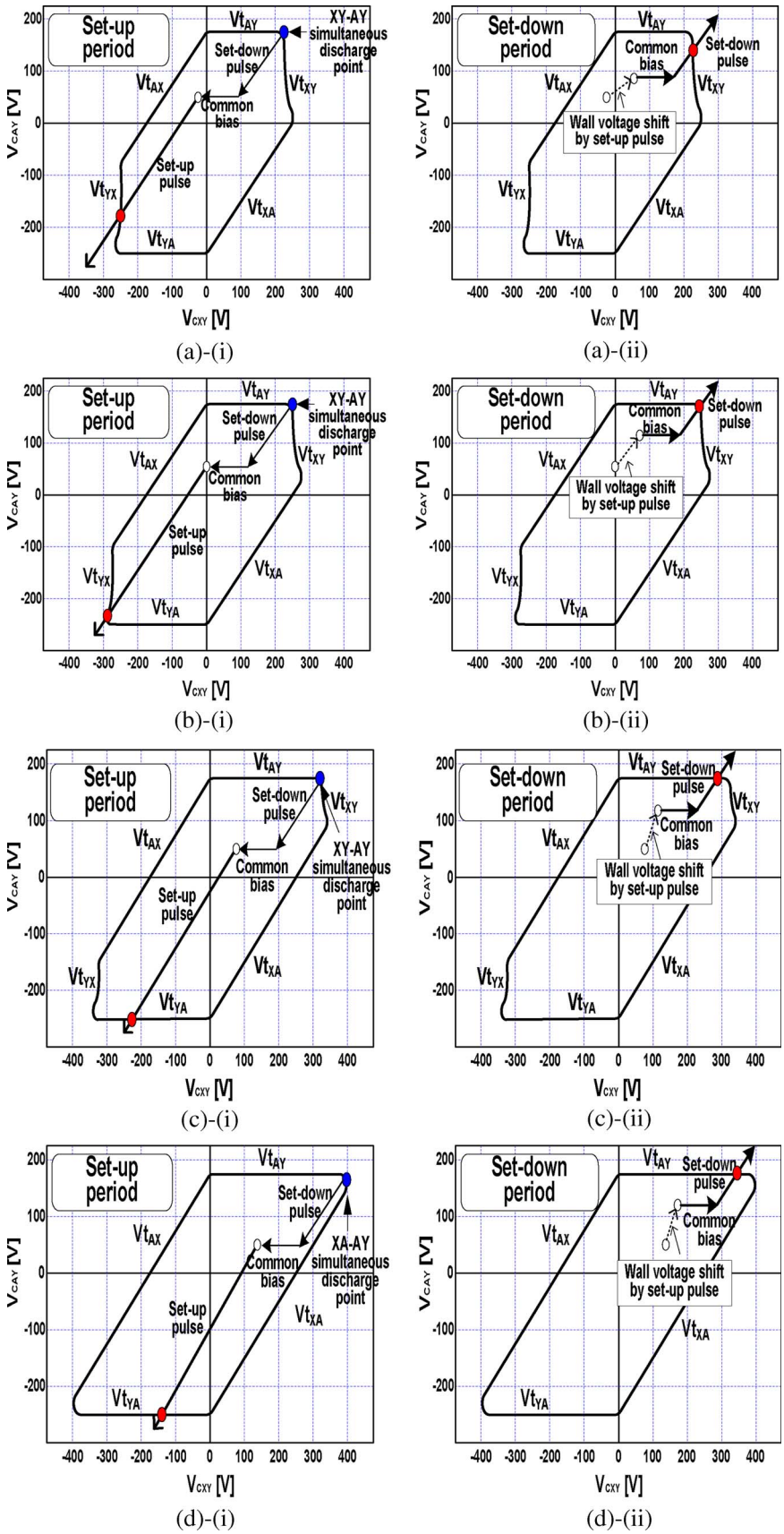

Fig. 5. Trajectories of cell voltage vectors displayed in V_t close-curves measured with various sustain gaps of (a) 50, (b) 100, (c) 200, and (d) 400 μm when 440 V set-up and -160 V set-down ramp voltages in Fig. 4 were applied to Y electrode, respectively.

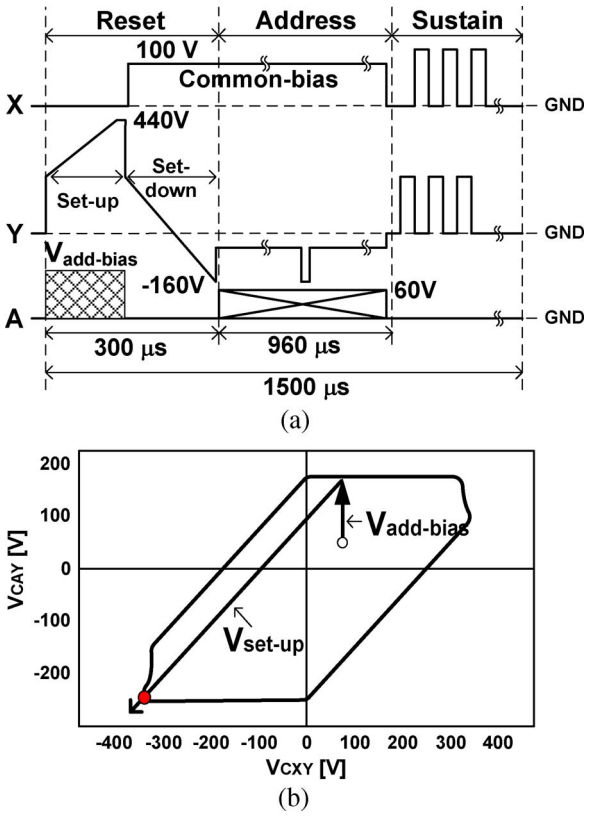

Fig. 6. (a) Modified reset waveform with $V_{\text{add-bias}}$ and (b) trajectories of voltage vector when $V_{\text{add-bias}}$ was applied to address (A) electrode with 200 μm wide-sustain-gap structure.

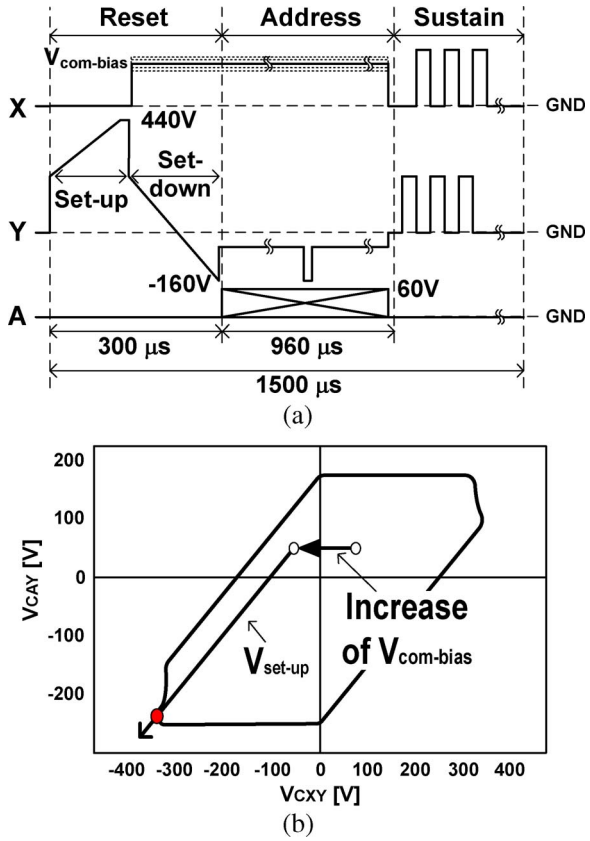

Fig. 7. (a) Modified reset waveform with $V_{\text{com-bias}}$ and (b) trajectories of voltage vector when $V_{\text{com-bias}}$ applied to X electrode was increased to higher level with 200 μm wide-sustain-gap structure.

weak reset discharge was produced. Consequently, with the 50 and 100 μm sustain gaps, stable reset discharge characteristics were observed. In contrast, with the 200 and 400 μm sustain gaps, the voltage vector exceeded V_{tYA} when a sufficient set-up voltage was applied, as shown in Fig. 5(c)-(i) and (d)-(i). In this case, since the A electrode protected by the phosphor layer acted as the cathode, as shown in Fig. 3(c)-(iv), an unstable reset discharge was produced. To suppress this unstable reset discharge, the cell voltage vector resulting from the set-up voltage should exceed V_{tYX} in the V_t close-curve. Thus, to exceed V_{tYX} with a 200 μm sustain gap, the cell voltage vector needed to be shifted up or the initial point of the cell voltage vector moved to the left. Fig. 5(a)-(ii), (b)-(ii), (c)-(ii), and (d)-(ii) shows the trajectories of the cell voltage vectors generated by the set-down ramp pulse of -160 V and the common bias pulse of 100 V after the initial point of the cell voltage vector was shifted by the set-up discharge. During a set-down period, the cell voltage vector exceeded V_{tXY} or V_{tAY} because the wall voltage generated by the set-up reset discharge was moved to upper and right direction, and the voltage vector by the set-down was also applied with upper and right direction, as shown in Fig. 5(a)-(ii), (b)-(ii), (c)-(ii), and (d)-(ii). As a result, although the sustain gap was wider, the XY- and AY-discharges were stably produced because the unstable discharge, i.e., XA-discharge was not be produced during the ramp set-down period.

Fig. 6(a) shows the modified reset waveform with $V_{\text{add-bias}}$ during the set-up period, while Fig. 6(b) shows the trajectory of the cell voltage vector when the modified reset waveform with $V_{\text{add-bias}}$ was applied in the case of a 200 μm wide-sustain-gap. When applying $V_{\text{add-bias}}$ to the A electrode during the ramp set-up period, the resultant cell voltage vector was shifted up and made contact with V_{tYX}, as shown in Fig. 6(b), resulting in a stable reset discharge.

Fig. 7(a) shows the modified reset waveform when varying the common bias voltage $(= V_{\text{com-bias}})$, while Fig. 7(b) shows the trajectory of the cell voltage vector when $V_{\text{com-bias}}$ was increased from 100 to 200 V with a 200 μm wide-sustain-gap structure. When increasing $V_{\text{com-bias}}$, more electrons were accumulated on the X and Y electrodes during a set-down period, thereby shifting the initial point of the cell voltage vector to the left, so the resultant cell voltage vector exceeded V_{tYX} of the V_t close-curve, as shown in Fig. 7(b). Consequently, a stable reset discharge was also obtained.

B. Effects of Two Parameters ($= V_{\text{add-bias}}$ and $V_{\text{com-bias}}$) on Off-Cells

Fig. 8 shows the changes in the IR waveforms emitted during the reset period when varying $V_{\text{add-bias}}$ and $V_{\text{com-bias}}$. When $V_{\text{add-bias}}$ was 0 V, and $V_{\text{com-bias}}$ was 100 V, lots of IR peaks were observed during the set-up period, due to the instability of the weak reset discharge caused by the non-MgO cathode condition. Meanwhile, when $V_{\text{add-bias}}$ was applied or $V_{\text{com-bias}}$ was increased, the cell voltage vector for the set-up ramp pulse

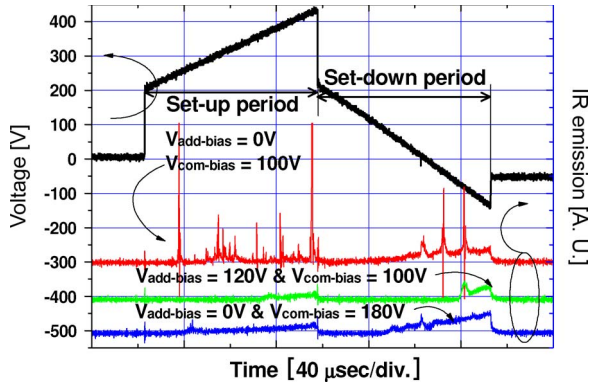

Fig. 8. Changes in IR emission during reset discharge when applying modified reset waveforms with various $V_{\text{add-bias}}$ and $V_{\text{com-bias}}$.

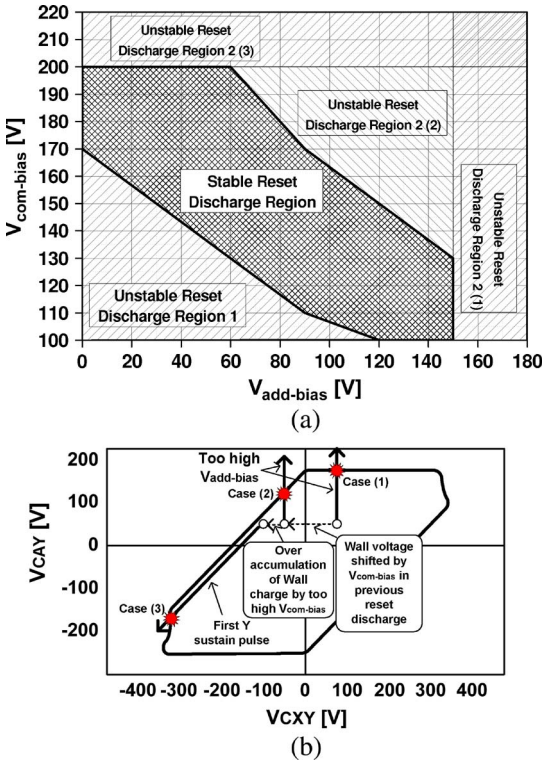

Fig. 9. (a) Stable and unstable reset discharge region relative to $V_{\text{add-bias}}$ and $V_{\text{com-bias}}$ with wide-sustain-gap ($= 200\ \mu$m) structure, and (b) V_t close-curve analysis in unstable reset discharge regions 1 and 2 in (a).

applied to the Y electrode exceeded V_{tYX} of the V_t close-curve, thereby reducing the peak and stabilizing the IR intensity, as shown in Fig. 8. With a $V_{\text{add-bias}}$ of 120 V and $V_{\text{com-bias}}$ of 100 V, a weak discharge was generated with a high set-up voltage, in comparison with the case of a $V_{\text{add-bias}}$ of 0 V and $V_{\text{com-bias}}$ of 180 V. As shown in Figs. 6 and 7, the addition of $V_{\text{add-bias}}$ or $V_{\text{com-bias}}$ enabled a weak reset discharge under an MgO cathode condition, resulting in a stable reset discharge even with a wide-sustain-gap structure.

Fig. 9(a) shows the stable and unstable reset discharge regions when varying the two parameters $V_{\text{add-bias}}$ and $V_{\text{com-bias}}$ with a wide-sustain-gap ($= 200\ \mu$m) structure. When increasing the amplitude of $V_{\text{com-bias}}$, the initial point in the V_t close-curve shifted to the left, while the cell voltage vector for the set-up ramp pulse moved close to V_{tYX}. Thus, the amplitude of

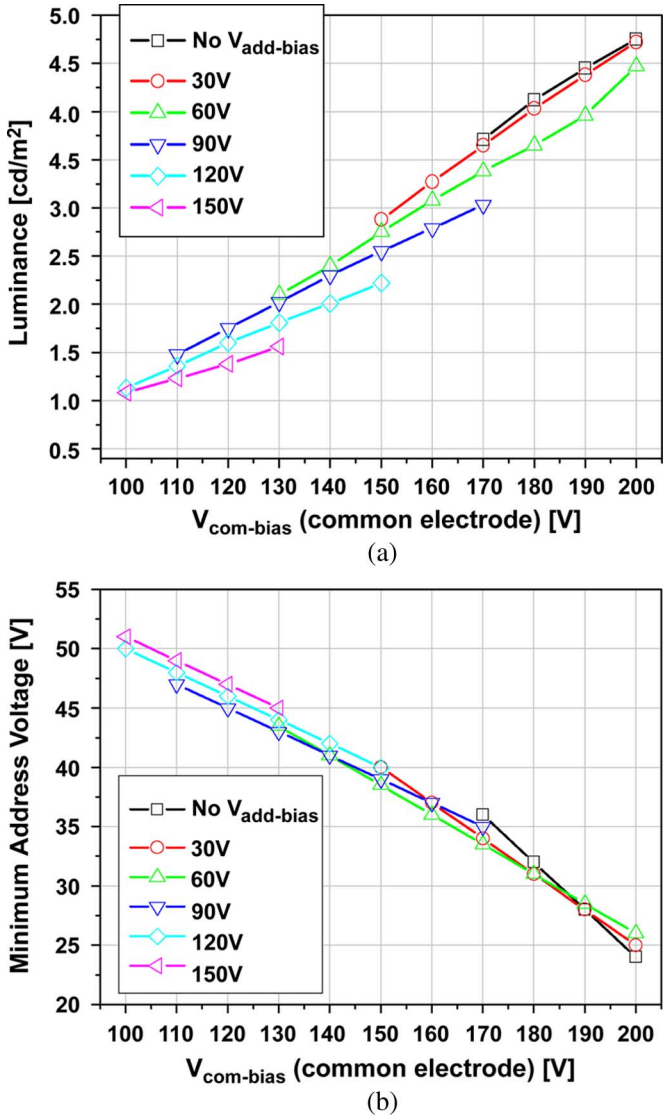

Fig. 10. (a) Changes in luminance during reset discharge and (b) minimum address voltage when applying various voltages of $V_{\text{add-bias}}$ and $V_{\text{com-bias}}$ with wide-sustain-gap ($= 200\ \mu$m) structure.

$V_{\text{add-bias}}$ was lowered as a result of applying $V_{\text{com-bias}}$ with a higher amplitude. In addition, increasing $V_{\text{com-bias}}$ with a wide-sustain-gap structure was favorable for the wall charge setup, as the same set-up reset voltage condition also facilitated a weak reset discharge. As shown in Fig. 9(a), a stable reset region was obtained at $V_{\text{add-bias}}$ (< 60 V) when increasing $V_{\text{com-bias}}$ above 130 V.

As shown in Fig. 9(a), two unstable reset discharge regions 1 and 2 were produced depending on the values of the two parameters $V_{\text{add-bias}}$ and $V_{\text{com-bias}}$. In unstable region 1, no misfiring discharge was produced during an address period, although an unstable reset discharge was produced by exceeding V_{tYA} in the V_t close-curve during the set-up period. On the other hand, in unstable region 2, a misfiring discharge was produced during a reset and sustain period. The schematic diagram of V_t close-curve was introduced in Fig. 9(b) to explain the misfiring problems during a reset and a sustain period, particularly under the unstable reset discharge region 2 of Fig. 9(a). In case (1) of Fig. 9(b), i.e., an unstable reset discharge region 2 (1) in

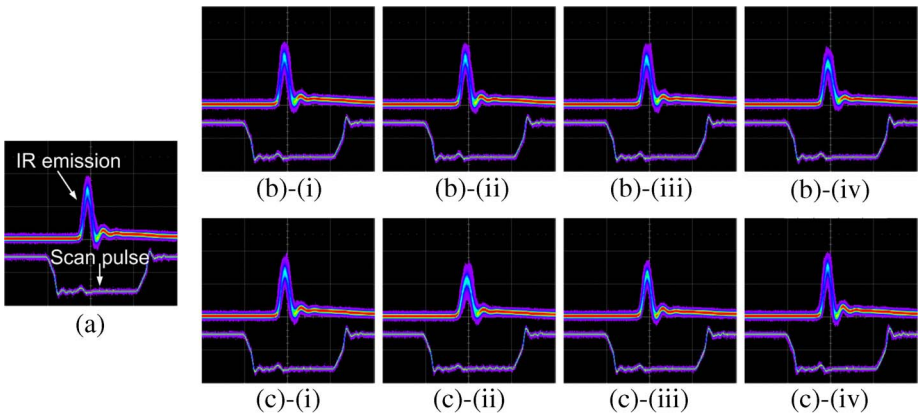

Fig. 11. Changes in IR waveforms emitted during address discharge when varying two parameters: $V_{\text{add-bias}}$ from 0 to 120 V and $V_{\text{com-bias}}$ from 100 to 180 V. (a) is reference ($V_{\text{add-bias}} = 0$ V, $V_{\text{com-bias}} = 100$ V), (b) (i) $V_{\text{add-bias}} = 30$ V, $V_{\text{com-bias}} = 100$ V, (ii) $V_{\text{add-bias}} = 60$ V, $V_{\text{com-bias}} = 100$ V, (iii) $V_{\text{add-bias}} = 90$ V, $V_{\text{com-bias}} = 100$ V, (iv) $V_{\text{add-bias}} = 120$ V, $V_{\text{com-bias}} = 100$ V, and (c) (i) $V_{\text{add-bias}} = 0$ V, $V_{\text{com-bias}} = 120$ V, (ii) $V_{\text{add-bias}} = 0$ V, $V_{\text{com-bias}} = 140$ V, (iii) $V_{\text{add-bias}} = 0$ V, $V_{\text{com-bias}} = 160$ V, (iv) $V_{\text{add-bias}} = 0$ V, $V_{\text{com-bias}} = 180$ V.

Fig. 9(a), the strong discharge between the A–Y electrodes was produced by exceeding V_{tAY} due to too high $V_{\text{add-bias}}$ (> 150 V), during a set-up period, whereas in case (2), i.e., unstable reset discharge region 2 (2), the strong discharge was produced between the A–X electrodes by exceeding V_{tAX} due to both high $V_{\text{add-bias}}$ (60–150 V) and $V_{\text{com-bias}}$ (130–200 V) during a set-up period. In case (3), i.e., unstable reset discharge region 2 (3), the sustain discharge was produced without an addressing discharge, because lots of wall charges were accumulated in off-cells due to too high $V_{\text{com-bias}}$ (> 200 V).

Fig. 10(a) and (b) shows the changes in (a) the luminance during the reset discharge and (b) the minimum address voltage relative to various voltages of $V_{\text{add-bias}}$ and $V_{\text{com-bias}}$. As such, when $V_{\text{add-bias}}$ was increased and $V_{\text{com-bias}}$ was simultaneously decreased, the luminance during the reset discharge was reduced to 1.08 cd/m^2, demonstrating that a high $V_{\text{add-bias}}$ and low $V_{\text{com-bias}}$ can suppress the background luminance produced by the reset waveform. As shown in Fig. 10(b), the subsequent address discharge was varied depending on the values of $V_{\text{add-bias}}$ and $V_{\text{com-bias}}$. When $V_{\text{add-bias}}$ was decreased and $V_{\text{com-bias}}$ was simultaneously increased, the minimum address voltage decreased to about 25 V. This result shows that the ensuing address discharge characteristics could be altered when varying $V_{\text{add-bias}}$ and $V_{\text{com-bias}}$. Therefore, the effects of various levels of $V_{\text{add-bias}}$ and $V_{\text{com-bias}}$ on the subsequent address and sustain discharge characteristics need to be investigated in detail. From the results in Figs. 9 and 10, the modified reset waveform with a $V_{\text{add-bias}}$ of 60 V and $V_{\text{com-bias}}$ of 130 V could be a good candidate for a stable reset discharge in a wide-sustain-gap of 200 μm. If a $V_{\text{add-bias}}$ with 120 V was applied to reduce the background luminance, the additional voltage source was needed in the address board because the address voltage for addressing required only 60 V. Consequently, $V_{\text{add-bias}}$ was reduced to 60 V to employ the modified reset waveform without additional cost. As for $V_{\text{add-bias}}$ of 60 V, a $V_{\text{com-bias}}$ was increased to 130 V for stable reset discharge. In that case, a stable reset discharge was obtained under a minimum background luminance of 2.1 cd/m^2.

C. Effects of Two Parameters ($= V_{\text{add-bias}}$ and $V_{\text{com-bias}}$) on On-Cells

To investigate the effects of the reset discharges under various $V_{\text{add-bias}}$ and $V_{\text{com-bias}}$ conditions on the on-cells with a wide-sustain-gap of 200 μm, the subsequent address discharge and first and second sustain discharge characteristics were examined under various $V_{\text{add-bias}}$ and $V_{\text{com-bias}}$ conditions. Fig. 11 shows the changes in the IR waveforms emitted during the address discharge when $V_{\text{add-bias}}$ was varied from 0 to 120 V and $V_{\text{com-bias}}$ varied from 100 to 180 V. Fig. 11(a) shows the IR emission during an address discharge with a $V_{\text{add-bias}}$ of 0 V and $V_{\text{com-bias}}$ of 100 V. Then, as shown in Fig. 11(b), when $V_{\text{add-bias}}$ was increased from 30 to 120 V at intervals of 30 V under a constant $V_{\text{com-bias}}$ of 100 V, the address discharge was observed to be weakened slightly. Fewer wall charges were also accumulated on the three electrodes due to the weak reset discharge with a higher $V_{\text{add-bias}}$, thereby slightly weakening the subsequent address discharge. With a constant $V_{\text{add-bias}}$ of 0 V, the address discharge was weakened until $V_{\text{com-bias}}$ was increased from 100 to 140 V, then with a $V_{\text{com-bias}}$ above 140 V, the address discharge was strengthened a little, as shown in Fig. 11(c). The minimum address voltage, i.e., the lowest voltage required for determining the on- or off-cell depended strongly on the wall voltage variation caused by $V_{\text{add-bias}}$ and $V_{\text{com-bias}}$. However, the result of Fig. 11 shows that under a sufficient address voltage, e.g., 60 V, the address discharge intensity slightly changes when varying the $V_{\text{add-bias}}$ and $V_{\text{com-bias}}$. Thus, for a wide-sustain-gap structure, the stability of the reset discharge was not found to have any serious effect on the subsequent address discharge, but rather played a significant role in the off-cells.

Fig. 12 shows the changes in the IR waveforms emitted during the first and second sustain discharges when $V_{\text{add-bias}}$ was varied from 0 to 120 V and $V_{\text{com-bias}}$ varied from 100 to 180 V. Fig. 12(a) shows the IR emission during the first and second sustain discharges with a $V_{\text{add-bias}}$ of 0 V and $V_{\text{com-bias}}$ of 100 V. Then, as shown in Fig. 12(b), when $V_{\text{add-bias}}$ was increased from 30 to 120 V at intervals of 30 V under a constant $V_{\text{com-bias}}$ of 100 V, the first sustain discharge was

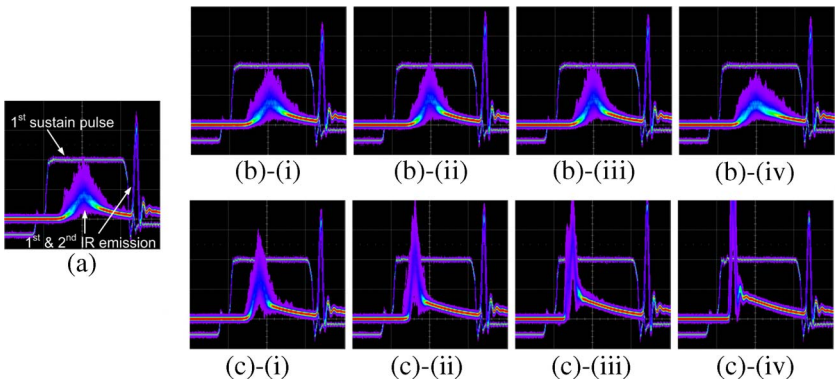

Fig. 12. Changes in IR waveforms emitted during first and second sustain discharges when varying two parameters: $V_{\text{add-bias}}$ from 0 to 120 V and $V_{\text{com-bias}}$ from 100 to 180 V. (a) is reference ($V_{\text{add-bias}} = 0$ V, $V_{\text{com-bias}} = 100$ V), (b) (i) $V_{\text{add-bias}} = 30$ V, $V_{\text{com-bias}} = 100$ V, (ii) $V_{\text{add-bias}} = 60$ V, $V_{\text{com-bias}} = 100$ V, (iii) $V_{\text{add-bias}} = 90$ V, $V_{\text{com-bias}} = 100$ V, (iv) $V_{\text{add-bias}} = 120$ V, $V_{\text{com-bias}} = 100$ V, and (c) (i) $V_{\text{add-bias}} = 0$ V, $V_{\text{com-bias}} = 120$ V, (ii) $V_{\text{add-bias}} = 0$ V, $V_{\text{com-bias}} = 140$ V, (iii) $V_{\text{add-bias}} = 0$ V, $V_{\text{com-bias}} = 160$ V, (iv) $V_{\text{add-bias}} = 0$ V, $V_{\text{com-bias}} = 180$ V.

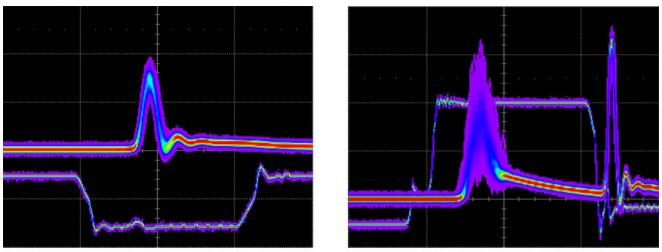

Fig. 13. IR waveforms emitted during (a) address and (b) first and second sustain discharge with $V_{\text{add-bias}}$ of 60 V and $V_{\text{com-bias}}$ of 130 V.

slightly weakened, yet the second sustain discharge recovered its normal intensity. As such, $V_{\text{add-bias}}$ did not influence the sustain discharge intensity, meaning that despite the variation from 30 to 120 V in $V_{\text{add-bias}}$, the wall charges necessary for the first sustain discharge had sufficiently accumulated. In contrast to the result in Fig. 12(b), Fig. 12(c) shows that the first sustain discharge intensity strongly depended on $V_{\text{com-bias}}$. With a constant $V_{\text{add-bias}}$ of 0 V, the first sustain was intensified when $V_{\text{com-bias}}$ was increased from 100 to 180 V. With a large value of $V_{\text{com-bias}}$, more wall charges were accumulated on the X and Y electrodes, although the address discharge intensity did not appear to change. Therefore, the resultant first sustain discharge was intensified under a high $V_{\text{com-bias}}$.

Fig. 13 shows the IR waveforms emitted during the address, first, and second sustain discharges with a $V_{\text{add-bias}}$ of 60 V and $V_{\text{com-bias}}$ of 130 V. Thus, for a wide-sustain-gap ($= 200$ μm) structure with a $V_{\text{add-bias}}$ of 60 V and $V_{\text{com-bias}}$ of 130 V, a stable reset discharge was obtained, followed by a strong first and second sustain discharge under a strong address discharge.

IV. Conclusion

For a wide-sustain-gap ($= 200$ μm) structure, a stable reset discharge under a low background luminance was examined relative to two parameters $V_{\text{add-bias}}$ and $V_{\text{com-bias}}$ applied during the reset period based on a V_t close-curve analysis. In addition, the effect of the same two parameters applied during the reset period on the on-cells, i.e., the address and first sustain discharges, was also examined in detail. As a result, when adjusting $V_{\text{add-bias}}$ to 60 V and $V_{\text{com-bias}}$ to 130 V, a stable reset discharge was obtained under a low background luminance, followed by a strong first and second sustain discharge under a strong address discharge.

References

[1] G. Oversluizen, M. Klein, S. de Zwart, S. van Heusden, and T. Dekker, "Discharge efficiency in plasma displays," *Appl. Phys. Lett.*, vol. 77, no. 7, pp. 948–950, Aug. 2000.

[2] J. D. Schemerhorn, E. Anderson, D. Levision, C. Hammon, J. S. Kim, B. Y. Park, J. H. Ryu, O. Shvydsky, and A. Sebastian, "A controlled lateral volume discharge for high luminous efficiency AC-PDP," in *Proc. SID Dig.*, 2000, pp. 106–109.

[3] L. F. Weber, "Positive column AC plasma display," U.S. Patent 618 484 8B1, Feb. 6, 2001.

[4] L. F. Weber, "Positive column AC plasma display," in *Proc. IDRC*, 2003, pp. 119–124.

[5] H. Kim and H.-S. Tae, "Firing and sustaining discharge characteristics in alternating current micro-discharge cell with three electrodes," *IEEE Trans. Plasma Sci.*, vol. 32, no. 2, pp. 488–492, Apr. 2004.

[6] K. C. Choi, N. H. Shin, K. S. Lee, B. J. Shin, and S.-E. Lee, "Study of various coplanar gaps discharges in AC plasma display panel," *IEEE Trans. Plasma Sci.*, vol. 34, no. 2, pp. 385–389, Apr. 2006.

[7] J. Y. Kim, H. Kim, H.-S. Tae, J.-H. Seo, and S.-H. Lee, "Effect of voltage distribution among three electrodes on microdischarge characteristics in AC-PDP with long discharge path," *IEEE Trans. Plasma Sci.*, vol. 34, no. 6, pp. 2579–2587, Dec. 2006.

[8] K. C. Choi, N. H. Shin, S. C. Song, J. H. Lee, and S. D. Park, "A new AC plasma display panel with auxiliary electrode for high luminous efficacy," *IEEE Trans. Electron Devices*, vol. 54, no. 2, pp. 210–218, Feb. 2007.

[9] C.-H. Park, D.-H. Kim, S.-H. Lee, J.-H. Ryu, and J.-S. Cho, "A new method to reduce addressing time in a large AC plasma display panel," *IEEE Trans. Electron Devices*, vol. 48, no. 6, pp. 1082–1086, Jun. 2001.

[10] J. K. Kim, J. H. Yang, W. J. Chung, and K.-W. Whang, "The addressing characteristics of an alternating current plasma display panel adopting a ramping reset pulse," *IEEE Trans. Electron Devices*, vol. 48, no. 8, pp. 1556–1563, Aug. 2001.

[11] C.-H. Park, S.-H. Lee, D.-H. Kim, J.-H. Ryu, and H.-J. Lee, "A modified ramp waveform to reduce reset period in AC plasma display panel," *IEEE Trans. Electron Devices*, vol. 49, no. 5, pp. 782–786, May 2002.

[12] C.-H. Park, S.-H. Lee, D.-H. Kim, J.-H. Ryu, and H.-J. Lee, "A new driving waveform to improve dark room contrast ratio in ac plasma display panel," *IEEE Trans. Electron Devices*, vol. 49, no. 7, pp. 1143–1150, Jul. 2002.

[13] G.-S. Kim, H.-Y. Choi, J.-H. Kim, and S.-H. Lee, "New reset waveform for the contrast ratio improvement of AC-PDP," *IEEE Trans. Electron Devices*, vol. 50, no. 7, pp. 1705–1708, Jul. 2003.

[14] J.-H. Ryu, J.-Y. Choi, H.-J. Lee, D.-H. Kim, H. J. Lee, and C.-H. Park, "Experimental observation and modified driving method to improve the high-temperature misfiring in AC PDP," *IEEE Trans. Electron Devices*, vol. 51, no. 12, pp. 2026–2032, Dec. 2004.
[15] B. J. Shin, K. C. Choi, and J. H. Seo, "Effects of pre-reset conditions on reset discharge from ramp reset waveforms in AC plasma display panel," *IEEE Trans. Electron Devices*, vol. 52, no. 1, pp. 17–22, Jan. 2005.
[16] B.-G. Cho and H.-S. Tae, "Reset-while-address (RWA) driving scheme for high-speed address in AC plasma display panel with high Xe content," *IEEE Trans. Electron Devices*, vol. 52, no. 11, pp. 2357–2364, Nov. 2005.
[17] B.-G. Cho, H.-S. Tae, K. Ito, J. W. Song, E. Y. Jung, J. C. Ahn, and N.-S. Jung, "A new driving waveform for improving luminous efficiency in AC PDP with large sustain gap under high Xe content," *IEEE Trans. Plasma Science*, vol. 34, no. 2, pp. 390–396, Apr. 2006.
[18] B. J. Shin, "Characteristics of an address discharge time lag in terms of a wall voltage in an AC PDP," *IEEE Trans. Electron Devices*, vol. 53, no. 7, pp. 1539–1542, Jul. 2006.
[19] K.-H. Park, S.-K. Jang, and H.-S. Tae, "Effects of various sustain gaps on reset discharge characteristics in AC-PDP," in *Proc. Eurodisplay Dig.*, 2005, pp. 68–71.
[20] K. Sakita, K. Takayama, K. Awamoto, and Y. Hashimoto, "High-speed address driving waveform analysis using wall voltage transfer function for three terminals and Vt close curve in three-electrode surface-discharge AC-PDPs," in *Proc. SID Dig.*, 2001, pp. 1022–1025.
[21] K. Sakita, K. Takayama, K. Awamoto, and Y. Hashimoto, "Ramp setup design technique in three-electrode surface-discharge AC-PDPs," in *Proc. SID Dig.*, 2002, pp. 948–951.
[22] K. Sakita, K. Awamoto, and Y. Hashimoto, "Applied voltage setting method and drive method of plasma display panel," U.S. Patent 654 542 3B2, Apr. 8, 2003.
[23] S. T. de Zwart and B. Salters, "Wall voltage fingerprint method in a three-electrode PDP cell," in *Proc. IDW Dig.*, 2001, pp. 845–848.
[24] H.-S. Tae, S.-K. Jang, K.-D. Cho, and K.-H. Park, "High-speed driving method using bipolar scan waveform in AC plasma display panel," *IEEE Trans. Electron Devices*, vol. 53, no. 2, pp. 196–204, Feb. 2006.
[25] J. Y. Kim and H.-S. Tae, "Analysis on discharge modes in AC plasma display panel with sustain gap of 200 μm," *IEEE Trans. Plasma Sci.*, vol. 35, no. 6, pp. 1766–1774, Dec. 2007.
[26] B. W. Byrum, Jr., "Surface aging mechanisms of AC plasma display panels," *IEEE Trans. Electron Devices*, vol. EDL-22, no. 9, pp. 685–691, Sep. 1975.

Ki-Hyung Park received the B.S. and M.S. degrees in electronic engineering from Kyungpook National University, Daegu, Korea, in 2002 and 2004, respectively, where he is currently working toward the Ph.D. degree.

His current research interests include the plasma physics and the driving waveform design of plasma display panels.

Heung-Sik Tae (M'00–SM'05) received the B.S., M.S., and Ph.D. degrees in electrical engineering from Seoul National University, Seoul, Korea, in 1986, 1988, and 1994, respectively.

Since 1995, he has been a Professor with the School of Electrical Engineering and Computer Science, Kyungpook National University, Daegu, Korea. His research interests include the optical characterization and driving waveform of plasma display panels.

Dr. Tae is a member of the Society for Information Display. He has been serving as an Editor for the IEEE TRANSACTIONS ON ELECTRON DEVICES section on display technology since 2005.

Jeong Hyun Seo received the B.S. degree in electrical engineering, and the M.S. and Ph.D. degrees in plasma engineering from Seoul National University, Seoul, Korea, in 1993, 1995, and 2000, respectively.

He was with the Plasma Display Panel (PDP) Division, Samsung SDI, Chonan, Korea, from 2000 to 2002, where his work focused on the design of driving pulses in ac PDP. Since September 2002, he has been a Professor with the Department of Electronics Engineering, University of Incheon, Incheon, Korea.